NMR Spectroscopy

International Edition: DOI: 10.1002/anie.201409888
German Edition: DOI: 10.1002/ange.201409888

Solid-State ^{17}O NMR Spectroscopy of Paramagnetic Coordination Compounds**

Xianqi Kong, Victor V. Terskikh, Rahul L. Khade, Liu Yang, Amber Rorick, Yong Zhang, Peng He, Yining Huang, and Gang Wu**

Abstract: *High-quality solid-state ^{17}O ($I = 5/2$) NMR spectra can be successfully obtained for paramagnetic coordination compounds in which oxygen atoms are directly bonded to the paramagnetic metal centers. For complexes containing V^{III} ($S = 1$), Cu^{II} ($S = 1/2$), and Mn^{III} ($S = 2$) metal centers, the ^{17}O isotropic paramagnetic shifts were found to span a range of more than 10000 ppm. In several cases, high-resolution ^{17}O NMR spectra were recorded under very fast magic-angle spinning (MAS) conditions at 21.1 T. Quantum-chemical computations using density functional theory (DFT) qualitatively reproduced the experimental ^{17}O hyperfine shift tensors.*

NMR signals from paramagnetic substances are generally more difficult to detect than those from diamagnetic compounds. This is because the hyperfine interactions between magnetic dipoles of unpaired electrons and atomic nuclei are substantially stronger than the typical nuclear spin interactions such as magnetic shielding, nuclear quadrupolar, and dipolar couplings. As a result, the NMR signals from paramagnetic compounds are significantly shifted and broadened compared with diamagnetic compounds. Despite experimental difficulties, solid-state NMR studies of paramagnetic compounds can be traced back to the early NMR studies on single crystals of $CuSO_4 \cdot 5H_2O$,[1] $CuCl_2 \cdot H_2O$,[2] and MnF_2.[3] In more recent years, there have been considerable interest in solution[4] and solid-state[5–16] NMR studies of organic and biological systems containing paramagnetic metal ions. To date, most NMR studies of paramagnetic compounds have relied on detection of ^1H and ^{13}C nuclei, because hydrogen and carbon atoms are generally remote from the paramagnetic metal centers, thus experiencing relatively weak hyperfine interactions. In contrast, as oxygen atoms are often directly bonded to the paramagnetic metal centers, ^{17}O NMR for paramagnetic coordination compounds is expected to be more challenging than the corresponding ^1H and ^{13}C NMR studies. Furthermore, the only NMR-active oxygen isotope, ^{17}O, has very low natural abundance (0.037 %) and its nuclear spin is quadrupolar ($I = 5/2$). In light of the recent advances in solid-state ^{17}O NMR studies of diamagnetic molecules including biological macromolecules,[17] we decided to explore the possibility of using solid-state ^{17}O NMR to study paramagnetic coordination compounds. We should note that solid-state ^{17}O NMR has been used previously to study ionic high T_c superconductors[18] and simple paramagnetic inorganic complexes.[19] The focus of our study is on solid-state ^{17}O NMR of paramagnetic coordination complexes containing organic ligands (that is, containing H, C, N, and O atoms).

We first examined two vanadium(III) ($S = 1$) complexes: $[V([^{17}O_2]acac)_3]$ and $K_3[V([^{17}O_4]oxalate)_3] \cdot 3H_2O$. Synthetic details for the preparation of ^{17}O-labeled paramagnetic coordination compounds are given in the Supporting Information. As seen in Figure 1, the static solid-state ^{17}O NMR spectrum for $[V([^{17}O_2]acac)_3]$ exhibits signals centered at around −1300 ppm and spanning over 1800 ppm. These spectral features are drastically different from those obtained for the diamagnetic analogue $[Al([^{17}O_2]acac)_3]$, which has the ^{17}O NMR signal at 270 ppm with a spectral span of only 400 ppm at 21.1 T.[20] For $[V([^{17}O_2]acac)_3]$, we were able to obtain a very fast MAS ^{17}O NMR spectrum in which all six crystallographically non-equivalent oxygen sites[21] are resolved. The ^{17}O isotropic shifts among the six directly bonded oxygen atoms differ by more than 500 ppm. In comparison, the isotropic ^{17}O chemical shifts for the six oxygen atoms in the diamagnetic $[Al([^{17}O_2]acac)_3]$ differ by only 5 ppm.[20] $K_3[V([^{17}O_4]oxalate)_3] \cdot 3H_2O$ is an interesting compound in which both direct chelating (O1, O2, O3) and non-bonding (O4, O5, O6) oxygen atoms are present.[22] As seen from Figure 1, the ^{17}O NMR signals from O1–O3 are found around −1200 ppm, whereas those from O4–O6 appear at 350 ppm. In diamagnetic metal oxalates, the ^{17}O NMR signals from chelating and non-bonding oxygen atoms typically differ by 40–70 ppm.[23]

[*] Dr. X. Kong, Prof. Dr. G. Wu
Department of Chemistry, Queen's University
Kingston, Ontario, K7L 3N6 (Canada)
E-mail: gang.wu@chem.queensu.ca
Dr. V. V. Terskikh
Department of Chemistry, University of Ottawa
Ottawa, Ontario, K1N 6N5 (Canada)
R. L. Khade, L. Yang, A. Rorick, Prof. Dr. Y. Zhang
Department of Chemistry, Chemical Biology, and Biomedical Engineering
Stevens Institute of Technology Castle Point on Hudson
Hoboken, New Jersey 07030 (USA)
E-mail: yong.zhang@stevens.edu
P. He, Prof. Dr. Y. Huang
Department of Chemistry, University of Western Ontario
London, Ontario, N6A 5B7 (Canada)

[**] This work was supported by NSERC of Canada. Y.Z. acknowledges the support from the National Institutes of Health (NIH) (GM085774). Access to the 900 MHz NMR spectrometer was provided by the National Ultrahigh Field NMR Facility for Solids (Ottawa, Canada), a national research facility funded by a consortium of Canadian universities, the Canada Foundation for Innovation, the Ontario Innovation Trust, Recherche Québec, and Bruker BioSpin and managed by the University of Ottawa (http://nmr900.ca).

Supporting information for this article is available on the WWW under http://dx.doi.org/10.1002/anie.201409888.

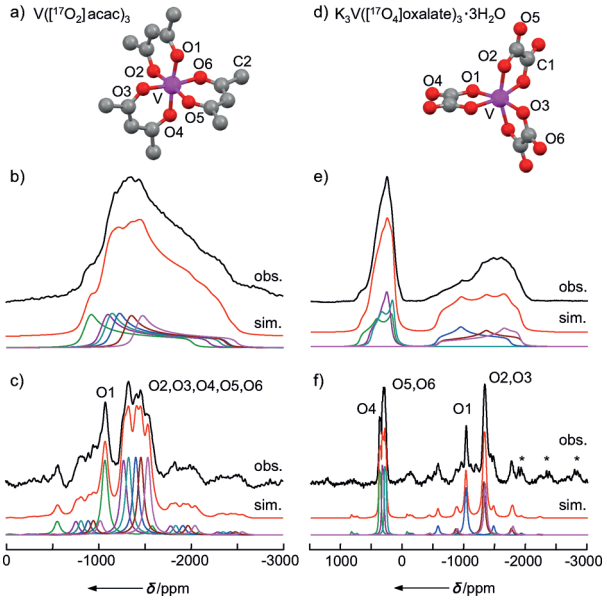

Figure 1. Molecular structures (a, d; hydrogen atoms are omitted for clarity), experimental and simulated static (b, e), and MAS (c, f) ^{17}O NMR spectra (21.1 T) of $[V([^{17}O_2]acac)_3]$ and $K_3[V([^{17}O_4]oxalate)_3]\cdot 3H_2O$. Simulated sub-spectra for individual sites are also shown. The sample spinning frequency was 62.5 and 55.0 kHz in (c) and (f), respectively. The signal numbering within either direct chelating or non-bonding oxygen atoms is arbitrary. ⋆ indicates the signal from the satellite transitions.

To properly analyze the experimental solid-state ^{17}O NMR spectra, a brief background theory is warranted. In paramagnetic compounds, the hyperfine interaction between nuclear and unpaired electron spins can be written as:

$$H_{\text{hyperfine}} = I \cdot \mathbf{A} \cdot S \tag{1}$$

where I and S are nuclear and electron spins, respectively, and $\mathbf{A}$ is the hyperfine interaction tensor. In general, the $\mathbf{A}$ tensor can be separated into the isotropic hyperfine coupling constant known as the Fermi contact shift A_{iso} and the anisotropic (traceless) dipolar tensor $\mathbf{T}$, that is:

$$\mathbf{A} = A_{\text{iso}} + \mathbf{T} \tag{2}$$

A_{iso} and $\mathbf{T}$ can be further expressed as:

$$A_{iso} = \frac{4\pi}{3S}\hbar\gamma_N g\mu_B\rho_{\alpha\beta} \tag{3}$$

$$T_{ij} = -\frac{1}{2S}\hbar\gamma_N g\mu_B\left\langle\frac{r^2\delta_{ij} - 3r_i r_j}{r^5}\right\rangle \tag{4}$$

where γ_N is the nuclear magnetogyric ratio, g is the free electron g-value, μ_B is the Bohr magneton, and $\rho_{\alpha\beta}$ is the electron spin density at the nucleus.

It is also known that under the condition of very rapid electron relaxation, the hyperfine interaction manifests itself in NMR spectra of a powder sample as a characteristic line shape identical to that due to the chemical shift anisotropy (CSA).[6] As a result, we can define a paramagnetic shift tensor containing both the orbital (from all paired electrons) and hyperfine (from unpaired electrons) contributions:

$$\delta_{ii} = \delta_{ii}^{\text{orb}} + \delta_{ii}^{\text{hf}} \tag{5}$$

where

$$\delta_{ii}^{\text{hf}} = \left(\frac{A_{ii}}{\hbar}\right)\frac{g\mu_B S(S+1)}{3\gamma_N kT} = \frac{m(S+1)}{T}\left(\rho_{\alpha\beta} + \frac{8\pi}{3}\rho_{\alpha\beta}^{ii}\right) \tag{6}$$

In Equation (6), $m = \mu_0(g\mu_B)^2/9k = 2.35\times10^7$ ppm K au^{-1} and $\rho_{\alpha\beta}^{ii}$ are the anisotropic spin dipolar tensor components in atomic units. For the paramagnetic shift tensor, we used the same convention for tensor components as that for the CS tensor for diamagnetic compounds, that is, $\delta_{11} > \delta_{22} > \delta_{33}$.

Along with the magnetic shielding and hyperfine interactions, ^{17}O nuclei in paramagnetic coordination complexes should also experience the same spin interactions as encountered in diamagnetic compounds (for example, quadrupolar and dipolar couplings). Therefore, the ^{17}O NMR spectrum from a paramagnetic compound is generally determined by the interplay of all the tensor interactions involved. A general analysis of the line shape for a powder sample can be quite complicated. Fortunately, at high magnetic fields (for example, 21.1 T), the spectral contribution from the ^{17}O paramagnetic shift tensor is much larger than those from other spin interactions. In this study, we were able to analyze the solid-state ^{17}O NMR spectra by considering only the paramagnetic shift tensor [Eq. (5)] and quadrupolar coupling tensor. Indeed, as seen from Figure 1, the ^{17}O NMR spectrum for each direct bonding oxygen site resembles the so-called CSA powder pattern.[6] For each compound, we typically analyzed ^{17}O NMR spectra obtained at two magnetic fields (Supporting Information, Figure S1).

Next we examined two copper(II) ($S = 1/2$) complexes: $[Cu([^{17}O_2]\text{-DL-alanine})_2]\cdot H_2O$ and $K_2[Cu([^{17}O_4]oxalate)_2]\cdot 2H_2O$. As seen from Figure 2, the ^{17}O NMR spectra of $[Cu([^{17}O_2]\text{-DL-alanine})_2]\cdot H_2O$ are surprisingly simple, in which only the signal from the non-bonding oxygen, O2, can be detected (for the full spectrum, see the Supporting Information, Figure S2). The O2 signal appears at 655 ppm, which is significantly shifted from the typical chemical shift, 250 ppm, observed for diamagnetic analogues. Similarly, the chelating oxygen atoms of the square-planar Cu^{II} complex $K_2[Cu([^{17}O_4]oxalate)_2]\cdot 2H_2O$ were also invisible in the spectra. However, one of the oxalate oxygen atoms, O1, which is directly coordinated to the Cu^{II} center as an axial ligand, exhibits an ^{17}O NMR signal at 240 ppm, which is not so different from those observed for diamagnetic metal oxalates.[23]

Here it is necessary to address the issue of observability of NMR signals in paramagnetic compounds. As Abragam explained in detail,[24] NMR signals may be observable only for nuclei for which the condition of $2\pi A\tau_e \ll 1$ holds, where A is the hyperfine coupling constant and τ_e is the averaged lifetime of electron spin in a given quantized state (generally equivalent to the electron spin-lattice relaxation time). This is the so-called fast relaxation/exchange limit. For mononuclear Cu^{II} complexes, τ_e is on the order of 10^{-9} s.[25] Typical A values

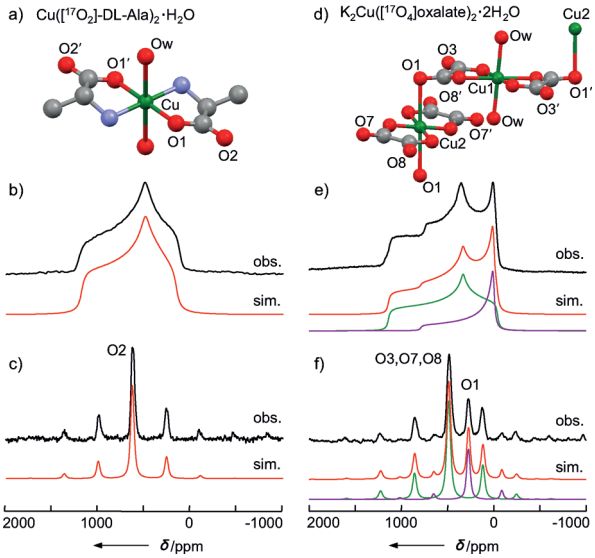

Figure 2. Molecular structures (a, d; hydrogen atoms are omitted for clarity), experimental and simulated static (b, e) and MAS (c, f) ^{17}O NMR spectra (21.1 T) of $[Cu([^{17}O_2]$-DL-alanine$)_2]\cdot H_2O$ and $K_2[Cu([^{17}O_4]oxalate)_2]\cdot 2H_2O$. Simulated sub-spectra for individual sites are also shown in (e) and (f). The sample spinning frequency was 45.0 kHz in (c) and (f). Note that the total signal integration for O3,O7,O8 is nearly three times of that for O1.

for chelating oxygen atoms in square-planar Cu^{II} complexes are ca. 50 MHz.[26] Thus, the fast exchange condition usually does not hold for a direct bonding oxygen in Cu^{II} complexes, making its signal too broad to be detected. Then why was the ^{17}O NMR signal for the direct chelating oxygen at the axial position in $K_2[Cu([^{17}O_4]oxalate)_2]\cdot 2H_2O$ observed? This is because in square-planar Cu^{II} complexes, the A value for the axial oxygen is distinctly small (ca. <0.2 MHz),[26] thus satisfying the fast-exchange condition.

The above success in detecting ^{17}O NMR signals in small Cu^{II} complexes led us to test whether the same approach can be extended to studies of more complex solid materials. To this end, we chose to examine $[Cu_3(BTC)_2(H_2O)_3]_n$ (BTC = benzenetricarboxylate) (also referred to as HKUST-1),[27] which is perhaps one of the most studied metal–organic frameworks. In our case, all carboxylate oxygen atoms in BTC are ^{17}O-labeled. As shown in Figure 3, the core structural motif is a dinuclear tetracarboxylate linker where the two Cu^{II} ions, separated by 2.628 Å,[27] are antiferromagnetically coupled. As a result, although the ground state of the

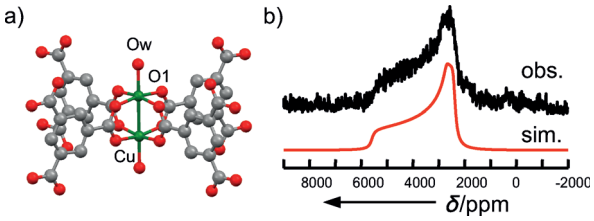

Figure 3. a) The two antiferromagnetically coupled Cu^{II} ions form the structural building block of the 3D framework in HKUST-1. Hydrogen atoms are omitted for clarity. b) Experimental and simulated static ^{17}O NMR spectra (14.1 T) of HKUST-1.

system has $S=0$, thus being diamagnetic, there exists a low-lying excited state with $S=1$. At 300 K, HKUST-1 exhibits considerable paramagnetism.[28] The ^{17}O NMR spectrum of HKUST-1 exhibits an isotropic paramagnetic shift of 3530 ± 100 ppm with the span being approximately 3100 ppm. This is the first time that ^{17}O NMR signals are detected in antiferromagnetically coupled dinuclear coordination complexes. This observation also suggests that the electron relaxation time in HKUST-1 must be much shorter than the typical value of 10^{-9} s, which is consistent with the previous observation of Bertini and co-workers[29] for dinuclear Cu^{II} compounds in solution.

Finally we examined $[Mn^{III}([^{17}O_2]acac)_3]$ ($S=2$). In agreement with the prediction from Equation (6), this $S=2$ system exhibits an exceedingly large paramagnetic shift (ca. 7500 ± 500 ppm) as well as a very large paramagnetic shift anisotropy (ca. 8000 ppm). As seen from the Supporting Information, Figure S3, as the entire ^{17}O NMR spectrum for the central transition spans close to 1 MHz, sufficient excitation cannot be achieved with a single RF pulse. Consequently, we acquired a variable offset cumulative spectrum (VOCS)[30] for this compound.

After obtaining high-quality solid-state ^{17}O NMR data for paramagnetic coordination compounds, we decided to test whether current computational methods can yield reliable results for ^{17}O hyperfine interactions. Several recent studies have shown that hyperfine shifts can be accurately computed for atoms that are not directly bonded to the paramagnetic metal center.[12,31] However, calculating ^{17}O hyperfine interactions for direct bonding oxygen atoms may be a greater challenge. After an extensive examination of various computational methods (Supporting Information), we found that the LC-wPBE approach produces the best computational results. As seen from Figure 4, the agreement is reasonable. These results suggest that the computation method can be used as a complementary method to aid the interpretation of experimental data. For example, the computational results made it possible to assign the ^{17}O NMR signals between direct chelating and non-bonding oxygen atoms. It is also interesting to note that both positive and negative ^{17}O paramagnetic shifts were observed for the direct chelating oxygen atoms. As Pritchard and Autschbach explained,[31g] the sign of the paramagnetic shift is related to the α/β spin balance in oxygen-to-metal σ donation. In Cu^{II} d^9 and Mn^{III} d^4 high-spin complexes, as the α-spin orbitals of the σ symmetry on the metal are occupied, only the β-spin orbital from the oxygen lone pair can contribute to the oxygen-to-metal σ bond, resulting in partial depletion of β-spin density (or α-spin surplus) at the oxygen nucleus. This leads to a positive ^{17}O paramagnetic shift. In V^{III} d^2 complexes, because the metal σ acceptor orbitals are empty, both α- and β-spin orbitals can accept the oxygen lone pair. However, the contribution from the metal α-spin orbital is slightly larger, which produces an excess of β-spin density at the oxygen nuclear site thus a negative ^{17}O paramagnetic shift. In this regard, our DFT calculations can in fact be used to provide easy visualization of the electron spin density distribution across the entire molecule (Supporting Information, Figure S5). Finally, while the general agreement between observed and calculated ^{17}O

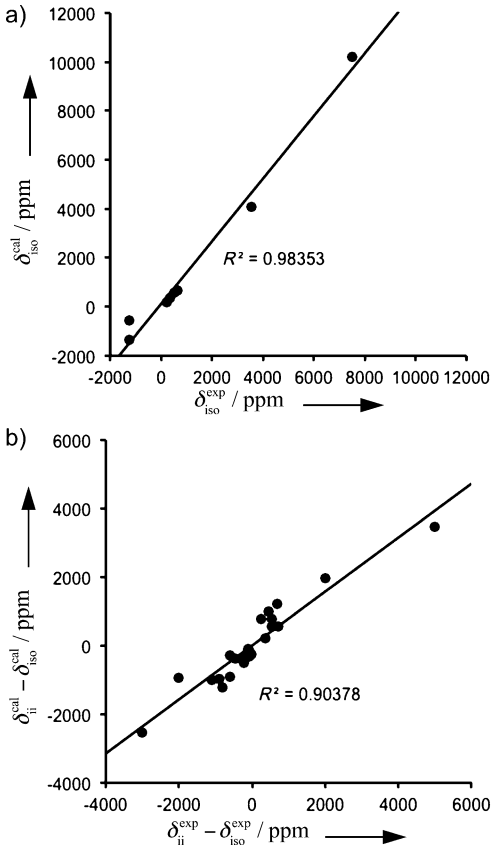

Figure 4. Comparison between experimental and calculated a) isotropic ^{17}O paramagnetic shifts and b) anisotropic paramagnetic shift tensor components.

paramagnetic shift tensors is reasonable over the 10000 ppm range, considerable discrepancies do exist for the direct chelating oxygen atoms, which have prevented us from making unambiguous signal assignment among structurally similar oxygen sites (for example, O1–O6 in $[V(acac)_3]$ and O1–O3 for $K_3[V(oxalate)_3]\cdot 3H_2O$). Possible sources for such discrepancies may include a) the neglect of other contributions to the paramagnetic shift tensors (for example, pseudocontact shift, bulk magnetic susceptibility, magnetic coupling among the paramagnetic metal centers, and zero-field splitting for systems with $S > 1/2$), b) inaccurate crystal structures, c) crystal packing effect, d) limitations of the current DFT methods, and e) large uncertainties in experimental data (for example, in $[Mn(acac)_3]$). Further investigations are clearly needed to address these issues.

In summary, we have shown that high-quality solid-state ^{17}O NMR spectra for various paramagnetic coordination compounds can be obtained, and experimental ^{17}O paramagnetic shift tensors were qualitatively reproduced by DFT computations. These results will inspire future interests in using solid-state ^{17}O NMR spectroscopy to study paramagnetic substances such as metalloproteins and related materials.

Keywords: coordination complexes · density functional calculations · hyperfine interactions · ^{17}O NMR spectroscopy · paramagnetism

How to cite: *Angew. Chem. Int. Ed.* **2015**, *54*, 4753–4757
Angew. Chem. **2015**, *127*, 4835–4839

[1] a) N. Bloembergen, *Physica* **1950**, *16*, 95–112; b) N. Bloembergen, N. J. Poulis, *Physica* **1950**, *16*, 915–919.
[2] N. J. Poulis, G. E. G. Hardeman, *Physica* **1952**, *18*, 201–220.
[3] R. G. Shulman, V. Jaccarino, *Phys. Rev.* **1957**, *108*, 1219–1231.
[4] a) I. Bertini, C. Luchinat, G. Parigi, *Solution NMR of Paramagnetic Molecules: Applications to Metallobiomolecules and Models*, Elsevier, Amsterdam, **2001**; b) T. E. Machonkin, W. M. Westler, J. L. Markley, *Inorg. Chem.* **2005**, *44*, 779–797; c) I. Bertini, C. Luchinat, G. Parigi, R. Pierattelli, *Dalton Trans.* **2008**, 3782–3790; d) G. Otting, *Annu. Rev. Biophys.* **2010**, *39*, 387–405.
[5] T. Sandreczki, D. Ondercin, R. W. Kreilick, *J. Am. Chem. Soc.* **1979**, *101*, 2880–2884.
[6] A. Nayeem, J. P. Yesinowski, *J. Chem. Phys.* **1988**, *89*, 4600–4608.
[7] A. R. Brough, C. P. Grey, C. M. Dobson, *J. Am. Chem. Soc.* **1993**, *115*, 7318–7327.
[8] K. Liu, D. Ryan, K. Nakanishi, A. E. McDermott, *J. Am. Chem. Soc.* **1995**, *117*, 6897–6906.
[9] Y. Ishii, N. P. Wickramasinghe, S. Chimon, *J. Am. Chem. Soc.* **2003**, *125*, 3438–3439.
[10] T. Jovanovic, A. E. McDermott, *J. Am. Chem. Soc.* **2005**, *127*, 13816–13821.
[11] N. P. Wickramasinghe, M. Shaibat, Y. Ishii, *J. Am. Chem. Soc.* **2005**, *127*, 5796–5797.
[12] G. Kervern, G. Pintacuda, Y. Zhang, E. Oldfield, C. Roukoss, E. Kuntz, E. Herdtweck, J.-M. Basset, S. Cadars, A. Lesage, C. Copéret, L. Emsley, *J. Am. Chem. Soc.* **2006**, *128*, 13545–13552.
[13] N. P. Wickramasinghe, M. A. Shaibat, C. R. Jones, L. B. Casabianca, A. C. de Dios, J. S. Harwood, Y. Ishii, *J. Chem. Phys.* **2008**, *128*, 052210.
[14] C. P. Jaroniec, *Solid State Nucl. Magn. Reson.* **2012**, *43–44*, 1–13.
[15] D. M. Dawson, L. E. Jamieson, M. I. H. Mohideen, A. C. McKinlay, I. A. Smellie, R. Cadou, N. S. Keddie, R. E. Morris, S. E. Ashbrook, *Phys. Chem. Chem. Phys.* **2013**, *15*, 919–929.
[16] S. Parthasarathy, Y. Nishiyama, Y. Ishii, *Acc. Chem. Res.* **2013**, *46*, 2127–2135.
[17] a) G. Wu, *Prog. Nucl. Magn. Reson. Spectrosc.* **2008**, *52*, 118–169; b) G. Wu, J. Zhu, X. Mo, R. Y. Wang, V. Terskikh, *J. Am. Chem. Soc.* **2010**, *132*, 5143–5155; c) J. Zhu, E. Ye, V. Terskikh, G. Wu, *Angew. Chem. Int. Ed.* **2010**, *49*, 8399–8402; *Angew. Chem.* **2010**, *122*, 8577–8580; d) J. Zhu, G. Wu, *J. Am. Chem. Soc.* **2011**, *133*, 920–932; e) X. Kong, L. A. O'Dell, V. Terskikh, E. Ye, R. Wang, G. Wu, *J. Am. Chem. Soc.* **2012**, *134*, 14609–14617; f) J. Zhu, T. Kurahashi, H. Fujii, G. Wu, *Chem. Sci.* **2012**, *3*, 391–397; g) X. Kong, M. Shan, V. Terskikh, I. Hung, Z. Gan, G. Wu, *J. Phys. Chem. B* **2013**, *117*, 9643–9654.
[18] a) C. Coretsopoulos, H. C. Lee, E. Ramli, L. Reven, T. B. Rauchfuss, E. Oldfield, *Phys. Rev. B* **1989**, *39*, 781–784; b) E. Oldfield, C. Coretsopoulos, S. Yang, L. Reven, H. C. Lee, J. Shore, O. H. Han, E. Ramli, D. Hinks, *Phys. Rev. B* **1989**, *40*, 6832–6849; c) F. Barriquand, P. Odier, D. Jerome, *Physica C* **1990**, *171*, 348–353; d) K. Ishida, H. Mukuda, Y. Kitaoka, K. Asayama, Z. Q. Mao, Y. Mori, Y. Maeno, *Nature* **1998**, *396*, 658–660; e) T. Imai, A. W. Hunt, K. R. Thurber, F. C. Chou, *Phys. Rev. Lett.* **1998**, *81*, 3006–3009; f) B. Chen, W. P. Halperin, P. Guptasarma, D. G. Hinks, V. F. Mitrovi, A. P. Reyes, P. L. Kuhns, *Nat. Phys.* **2007**, *3*, 239–242.
[19] a) W. J. Looyestijn, T. O. Klaassen, N. J. Poulis, *Physica B* **1978**, *93*, 349–357; b) A. Olariu, P. Mendels, F. Bert, F. Duc, J. C. Trombe, M. A. de Vries, A. Harrison, *Phys. Rev. Lett.* **2008**, *100*, 087202.

[20] A. Wong, M. E. Smith, V. Terskikh, G. Wu, *Can. J. Chem.* **2011**, *89*, 1087 – 1094.
[21] K. Min, A. L. Rhinegold, J. S. Miller, *Inorg. Chem.* **2005**, *44*, 8433 – 8441.
[22] M. A. Viswamitra, *Z. Kristallogr.* **1962**, *117*, 437 – 449.
[23] A. Wong, G. Thurgood, R. Dupree, M. E. Smith, *Chem. Phys.* **2007**, *337*, 144 – 150.
[24] A. Abragam, *The Principles of Nuclear Magnetism*, Oxford University Press, London, UK, **1961**.
[25] L. Banci, I. Bertini, C. Luchinat, *Nuclear and Electronic Relaxation. The magnetic nuclear-unpaired electron coupling in solution*, VCH, Weinheim, **1991**.
[26] W. B. Lewis, M. Alei, L. O. Morgan, *J. Chem. Phys.* **1966**, *45*, 4003 – 4013.
[27] S. S.-Y. Chui, S. M.-F. Lo, J. P. H. Charmant, A. G. Orpen, I. D. Williams, *Science* **1999**, *283*, 1148 – 1150.
[28] X. X. Zhang, S. S.-Y. Chui, I. D. Williams, *J. Appl. Phys.* **2000**, *87*, 6007 – 6009.
[29] N. N. Murthy, K. D. Karlin, I. Bertini, C. Luchiant, *J. Am. Chem. Soc.* **1997**, *119*, 2156 – 2162.
[30] D. Massiot, I. Farnan, N. Gautier, D. Trumeau, A. Trokiner, J. P. Coutures, *Solid State Nucl. Magn. Reson.* **1995**, *4*, 241 – 248.
[31] a) S. J. Wilkens, B. Xia, F. Weinhold, J. L. Markley, W. M. Westler, *J. Am. Chem. Soc.* **1998**, *120*, 4806 – 4814; b) J. Mao, Y. Zhang, E. Oldfield, *J. Am. Chem. Soc.* **2002**, *124*, 13911 – 13920; c) Y. Zhang, H. H. Sun, E. Oldfield, *J. Am. Chem. Soc.* **2005**, *127*, 3652 – 3653; d) Y. Zhang, E. Oldfield, *J. Am. Chem. Soc.* **2008**, *130*, 3814 – 3823; e) Y. Ling, Y. Zhang, *J. Am. Chem. Soc.* **2009**, *131*, 6386 – 6388; f) J. Autschbach, S. Patchkovskii, B. Pritchard, *J. Chem. Theory Comput.* **2011**, *7*, 2175 – 2188; g) B. Pritchard, J. Autschbach, *Inorg. Chem.* **2012**, *51*, 8340 – 8351.

Received: October 8, 2014
Published online: February 18, 2015

